Electronic Supplementary Information

Structural Transitions during the Water Sorption Process in two Layered Metal Hydrogen-Bonded Organic Frameworks and the Effect of the H-Bonds Strength between the Layers

Patrice Kenfack Tsobnang*[a], Yannick Thiery Sakam Nchedoung [a], Dominik Fröhlich[b], Florence Porcher [c], Lina Rustam[b], Emrah Hastürk[d], Christoph Janiak*[d]

[a] *University of Dschang, Department of Chemistry, PO Box 67, Dschang, Cameroon,*

[b] *Fraunhofer-Institut for Solar Energy Systems ISE, Division Thermal Systems and Buildings, Heidenhofstraße 2, 79110 Freiburg, Germany,*

[c] *Laboratoire Léon Brillouin (LLB), UMR 12 CEA/CNRS, Bât. 563 CEA Saclay, 91191 Gif-sur-Yvette cedex, France*

[d] *Institut für Anorganische Chemie und Strukturchemie, Heinrich-Heine-Universität Düsseldorf, Universitätsstraße 1, 40225 Düsseldorf, Germany,*

* Corresponding authors. E-mail addresses: patrice.kenfack@univ-dschang.org, pakenfack@gmail.com (P. K. Tsobnang); janiak@uni-duesseldorf.de (C. Janiak)

Section 1. Packing diagrams and characteristics of the Hydrogen bonds of I' and II'

Table S1. Hydrogen bonds length (in Å) and angles (°) for **I'**[1]

Packing direction	D-H...A	d(D-H) Å	d(H...A) (Å)	d(D...A) (Å)	(DHA) (°)
a axis	N(6)-H(6B)...O(1)^{iv}	0.79(9)	2.13(9)	2.910(8)	170(9)
	N(4)-H(4B)...O(11)^{ii}	0.90	2.02	2.837(7)	150.7
	N(3)-H(3A)...O(11)^{ii}	0.88(8)	2.23(8)	2.901(8)	133(7)
c axis	N(4)-H(4A)...O(10)^{i}	0.90	1.85	2.718(7)	160.1
	N(6)-H(6A)...O(10)^{i}	0.87(8)	2.32(8)	3.130(9)	155(7)
	N(6)-H(6A)...O(9)^{i}	0.87(8)	2.57(8)	3.246(9)	136(7)
b axis	C(9)-H(9)...O(3)^{v}	0.93	2.48	3.150(7)	128.5
	N(3)-H(3B)...O(8)^{iii}	0.86(8)	2.05(9)	2.777(8)	141(8)

Symmetry codes : i) x, y, z-1 ii) x-1/2,-y+1/2, z-1/2 iii) -x,-y,-z+1 iv) x+1/2,-y+1/2, z-1/2 v) -x+1/2, y+1/2,-z+3/2

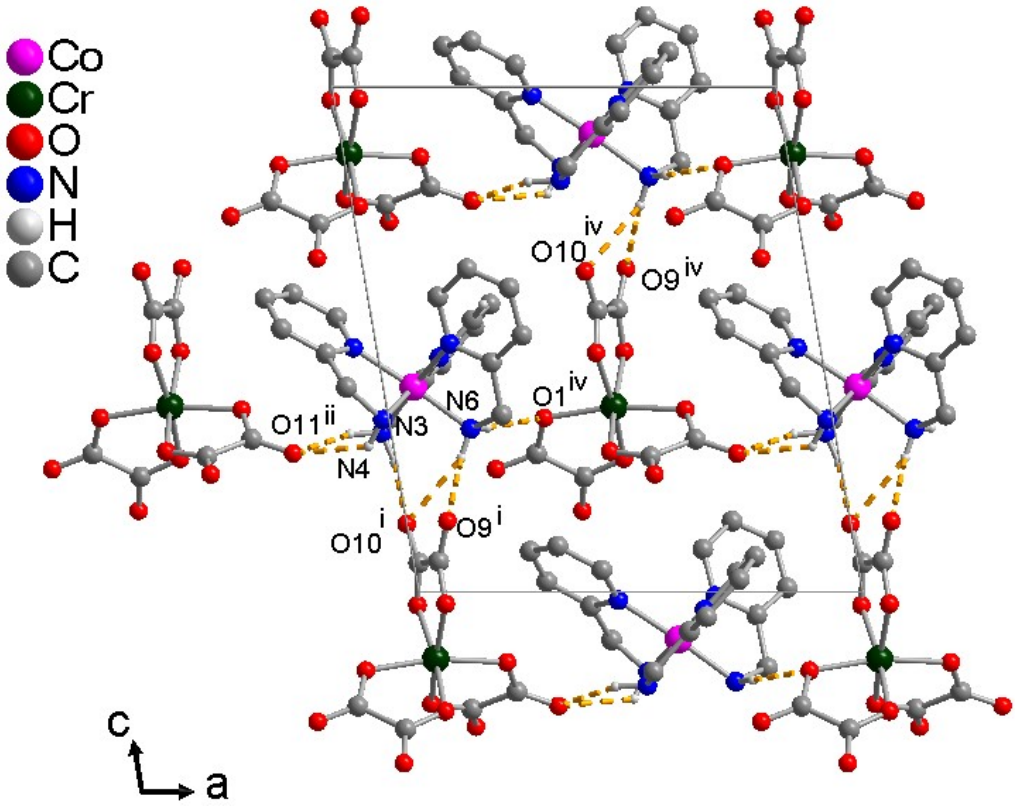

(a)

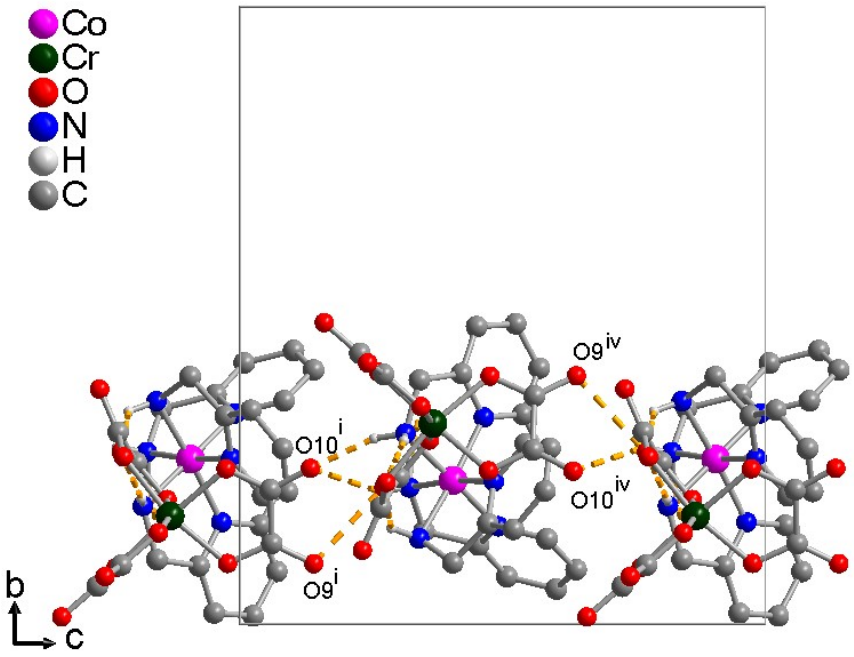

(b)

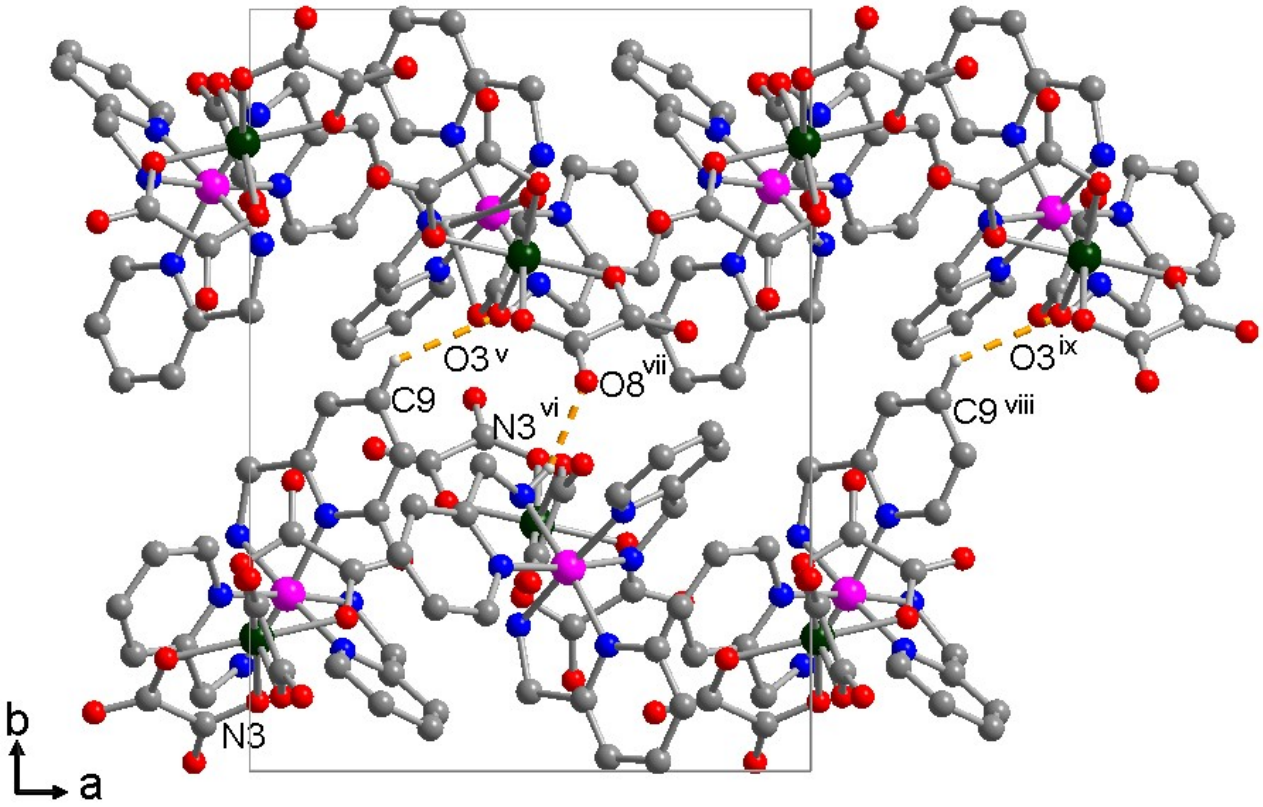

(c)

Figure S1. Diagrams showing: **(a)** the packing of the ionic units of **I'** to build a layer in the *ac* plane, **(b)** a layer of **I'** in the *bc* plane **(c):** the stacking of two consecutive layers of **I'** along the *b axis direction.*

The Hydrogen bonds in this packing are drawn with light orange color and for clarity, only the hydrogen atoms involved in these hydrogen bonds are shown.

See Table S1 for symmetry codes. Additional codes: vi: x + ½, - y + ½, z + ½; vii: - x + ½, y + ½, – z + 3/2; viii: x +1, y, z; ix: - x + 3/2, y + ½, - z + 3/2.

Table S2. Hydrogen bonds length (in Å) and angles (°) for **II' [2]**

Packing direction	D-H...A	d(D-H) Å	d(H...A) (Å)	d(D...A) (Å)	(DHA) (°)
c axis	N6—H6B···O5	0.86 (6)	2.16 (6)	2.915 (6)	145 (5)
	N8—H8B···O3	0.82 (6)	2.20 (6)	2.966 (5)	155 (5)
	N3—H3B···O12	0.90 (5)	2.25 (5)	3.023 (5)	143 (4)
	N1—H1A···O6	0.89 (6)	2.06 (6)	2.916 (6)	161 (5)
a axis	N6—H6A···O9^{ii}	0.94 (6)	2.44 (6)	3.205 (6)	139 (5)
	C13—H13···O9^{ii}	0.93	2.50	3.326 (6)	148
	C14—H14···O8^{ii}	0.93	2.60	3.517 (6)	170
	C26—H26···O4^{iv}	0.93	2.52	3.277 (7)	139
b axis	O1W—H2W···O6^{v}	0.87	2.18	3.017 (6)	161.3
	O1W—H1W···O2^{iv}	0.98	2.06	3.011 (7)	164.9
	N1—H1B···O1W	1.02 (6)	2.04 (6)	3.038 (7)	165 (5)
	N8—H8A···O1^{i}	0.82 (6)	2.25 (6)	3.012 (6)	157 (5)
	N3—H3A···O10^{i}	0.88 (5)	2.19 (5)	2.973 (5)	147 (4)
	C22—H22···O1^{iii}	0.93	2.32	3.033 (7)	134

Symmetry codes : (i) –x +1, -y, -z +1; (ii) x -1/2, -y +1/2, z+1/2; (iii) -x+1/2, y +1/2, -z +3/2; (iv) x+1/2, -y+1/2, z -1/2; (v) -x+1, -y+1, -z; (vi) x, y, z+1.

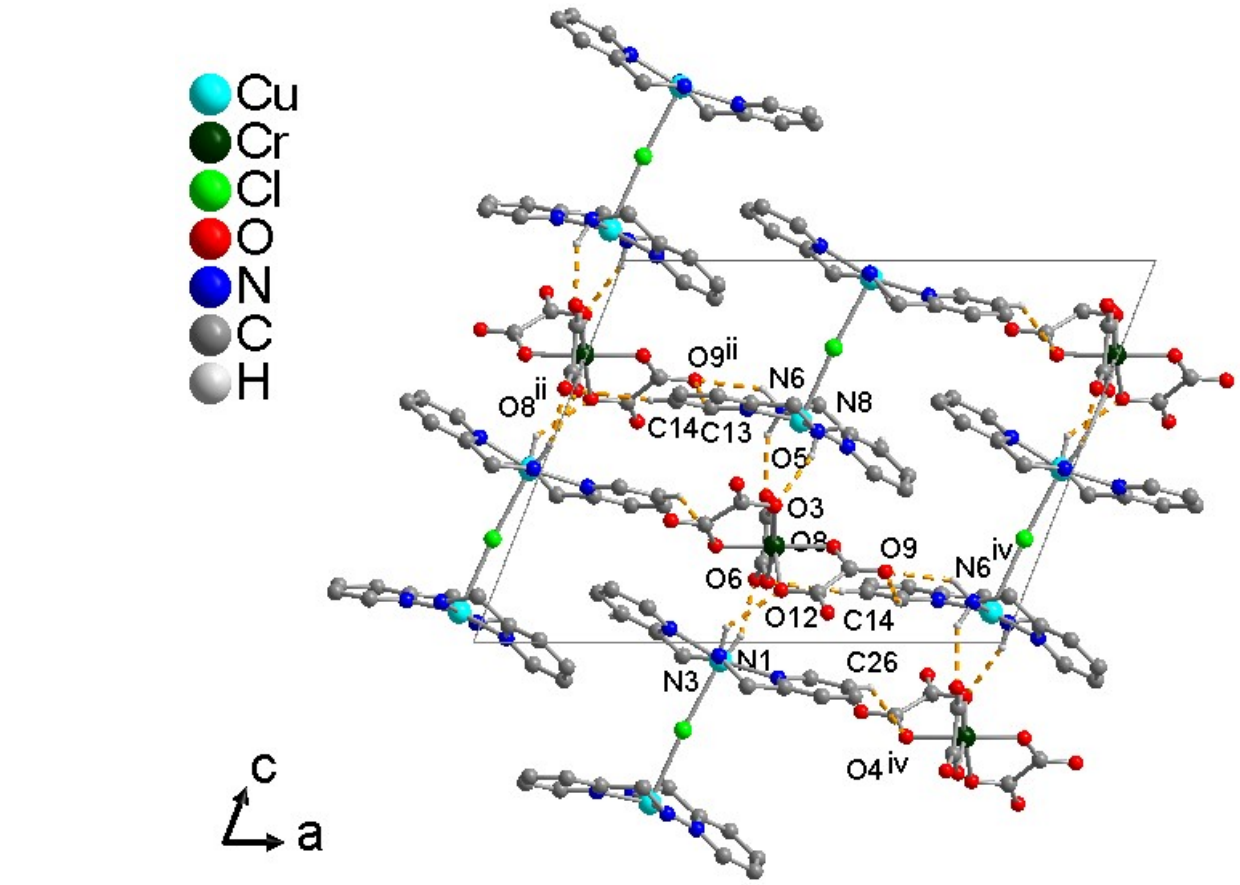
Cu
Cr
Cl
O
N
C
H
O9ii
N6
O8ii
N8
C14
C13
O5
O3
O8
O9
N6iv
O6
O12
C14
N1
C26
N3
O4iv
c
a

(a)

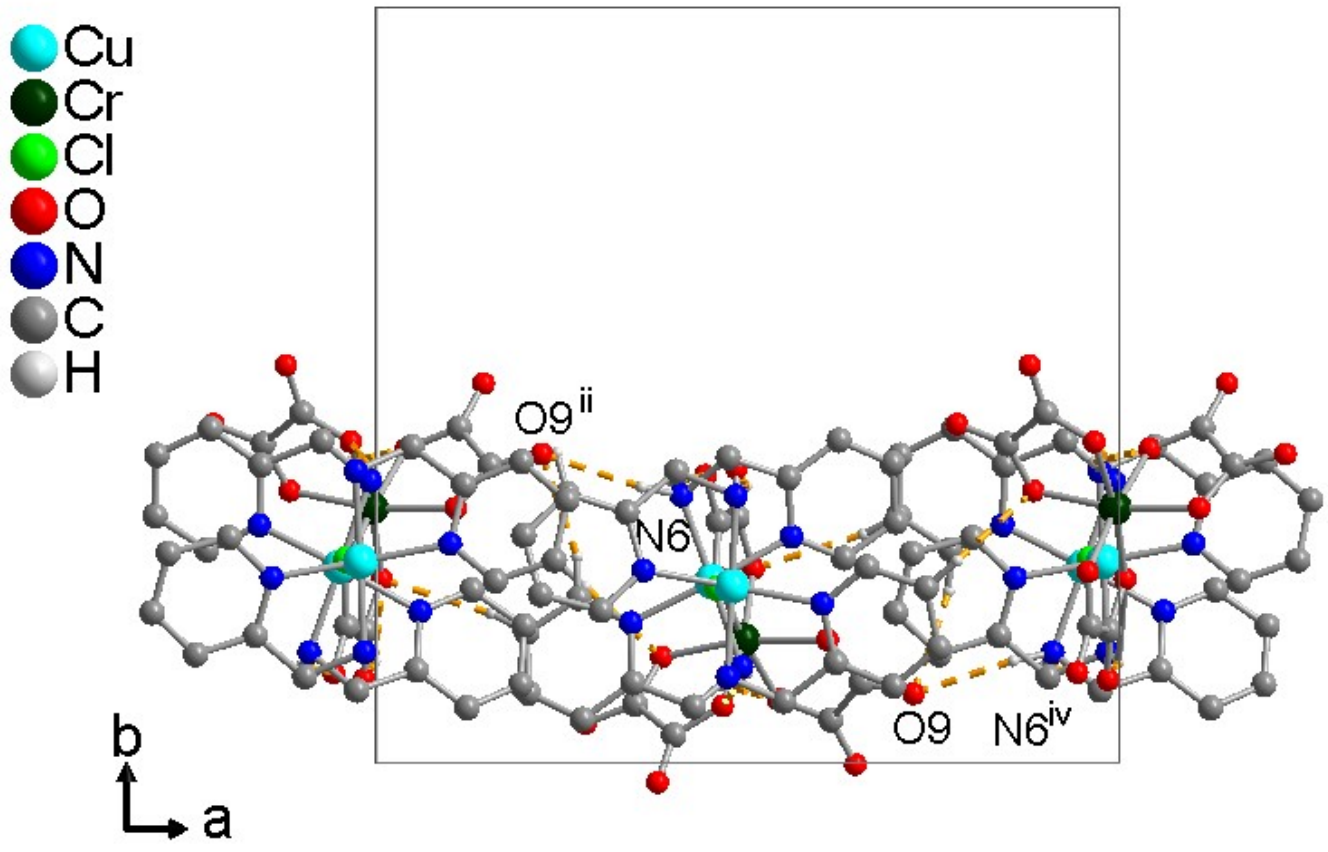
Cu
Cr
Cl
O
N
C
H
O9ii
N6
O9
N6iv
b
a

(b)

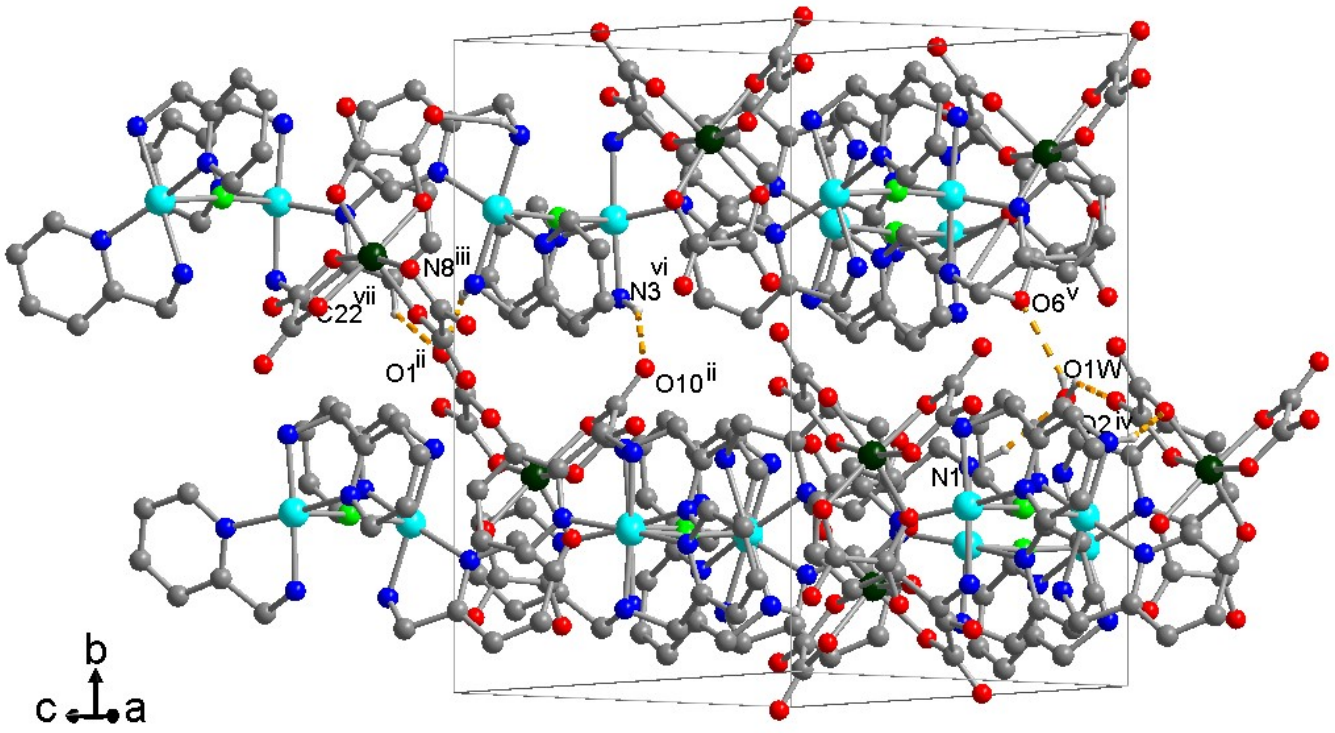

(c)

Figure S2. Diagrams showing: **(a)** the packing of units of **II'** to build a layer in the *ac* plane, **(b)** a layer of **II'** along the *b axis direction* and **(c):** the stacking along the *b axis direction* of two consecutive layers of **II'**.

The Hydrogen bonds in this packing are drawn with light orange color and for clarity, only the hydrogen atoms involved in these hydrogen bonds are shown.

See Table S2 for symmetry codes. Additional codes: vi: - x + ½, y + ½, -z + ½; vii: - x, - y + 1, – z + 1.

Section 2. Synthesis of $[Co(amp)_3][Cr(ox)_3] \cdot 6H_2O$ (I) and $[Cu_2(amp)_4Cl][Cr(ox)_3]\cdot 6H_2O$ (II)

Apart from the compound $K_3Cr(ox)_3\cdot 3H_2O$ which has been previously synthesized, all the other reagents used in this work are all from commercial sources and were used without any treatment. The list of these chemical are: potassium oxalate monohydrate ($K_2C_2O_4.H_2O$, 99%, Sigma- Aldrich), oxalic acid dihydrate ($H_2C_2O_4\cdot 2H_2O$, 99.9%, Fisher Scientific International Company), potassium dichromate ($K_2Cr_2O_7$, 99%, ABSEQ company LTD), cobalt chloride hexahydrate ($CoCl_2\cdot 6H_2O$, 98.9%, Sigma-Aldrich), 2-picolyamine ($C_6H_8N_2$, 98.0%, Sigma-Aldrich), and Copper chloride dihydrate ($CuCl_2\cdot 2H_2O$, 99%, Sigma-Aldrich). The synthesis of $K_3Cr(ox)_3\cdot 3H_2O$ has been done by dissolving 10.55 g (62 mmol) of $K_2C_2O_4\cdot H_2O$ crystals in preheated distilled water and the solution obtained is left under magnetic stirring for three minutes. Then, 27.5 g (22 mmol) of $H_2C_2O_4\cdot 2H_2O$ were added in small portions. After total dissolution, 9.5 g (32 mmol) of $K_2Cr_2O_7$ added in small portions. The reaction mixture was left under strong thermal stirring for 45 min at a temperature of 80 ° C. The solution obtained was filtered and left for slow evaporation for ten days. 28.36 g of large elongated crystals, of purple-blue color of $K_3Cr(ox)_3\cdot 3H_2O$ (yield of 91%) in agreement with the literature were obtained.

For the synthesis of $[Co(amp)_3][Cr(ox)_3]$ **(I)**, 1.57 g (3.22 mmol) of $K_3Cr(ox)_3\cdot 3H_2O$ previously synthesized were dissolved in 10ml of water at 60 °C and 15 min later, the mixture of 0.77 g (3.2 mmol) of $CoCl_2\cdot 6H_2O$ and 1 mL (9.7 mmol) of 2-picolylamine was added. The solution was stirred for 20 minutes at 60 °C then filtered and concentrated by slow evaporation of the solvent under ambient air. After 6 days, brown crystals of **(I)** were obtained from this solution. These crystals were filtered, washed with water and acetone. For $[Cu_2(amp)_4Cl][Cr(ox)_3]\cdot 1H_2O$ (**II**), 0.28 g (1.64 mmol) of $CuCl_2\cdot 2H_2O$ were dissolved in 10 mL of water and 0.5 mL (4.94 mmol) of 2-picolylamine was added. The solution was stirred for 15 minutes at 60 ° C and before adding a solution of $K_3Cr(C_2O_4)_3\cdot 3H_2O$ obtained by dissolving 0.76 g of the compound (1.64 mmol) in 10 mL of water at 60 °C. The mixture was stirred for 30 minutes at this temperature, then filtered and concentrated by slow evaporation of the solvent in ambient air. A filtrate formed one week later blue crystals of prismatic shape with a yield of 71% in agreement with the literature.

Section 3: Crystal data of the materials and confirmation of the synthesis of I and II.

Table S3. Crystal data for **I', I, II'** and **II** [1, 2]

	I'	**I**	**II'**	**II**
Chemical formula	$[Co(amp)_3]$ $[Cr(ox)_3]$	$[Co(amp)_3]$ $[Cr(ox)_3]\cdot 6H_2O$	$[Cu_2(amp)_4Cl]$ $[Cr(ox)_3]\cdot 1H_2O$	$[Cu_2(amp)_4Cl]$ $[Cr(ox)_3]\cdot 6H_2O$
Crystal system, space group	Monoclinic, $P2_1/n$	Monoclinic, $P2_1/n$	Monoclinic, $P2_1/n$	Monoclinic, $C2/c$
a(Å)	12.002(3)	13.2467(7)	17.568(5)	17.5980(5)
b(Å)	16.051(4)	18.2864(10)	16.601(5)	18.3030(5)
c (Å)	13.853(4)	14.1403(6)	13.578(5)	13.8200(4)
β (°)	99.754(6)	100.017(2)	68.486(5)	113.671(1)
Volume ($Å^3$)	2630.0(13)	4108.5(3)	3684(2)	4076.9(2)

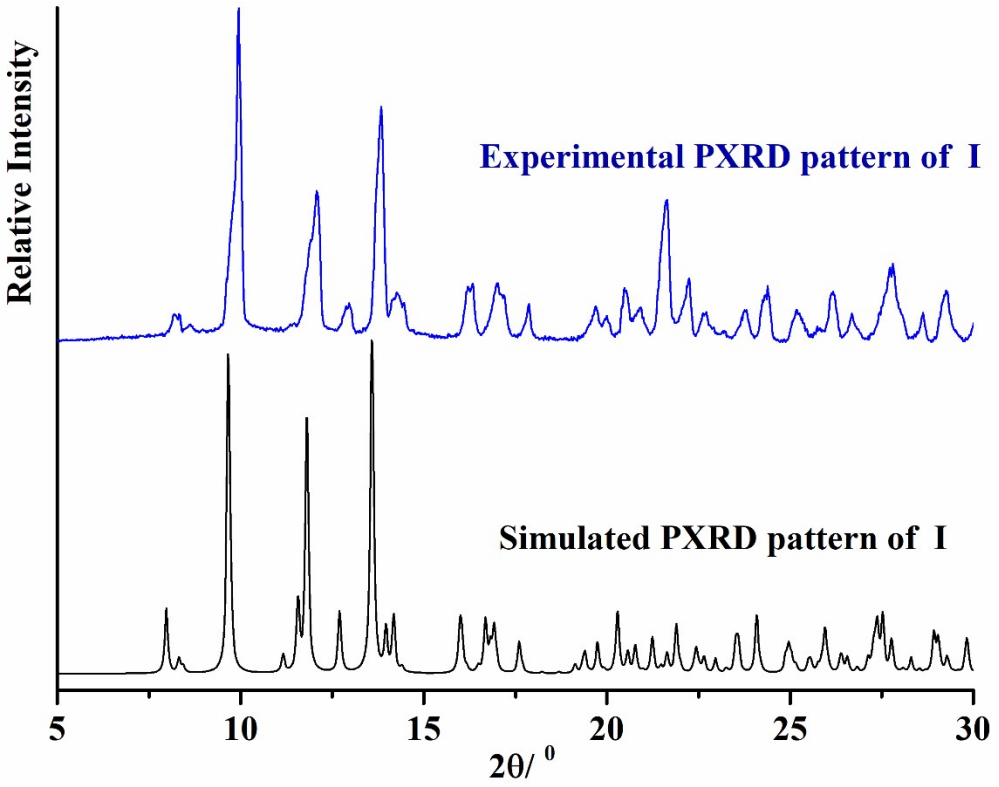

(a)

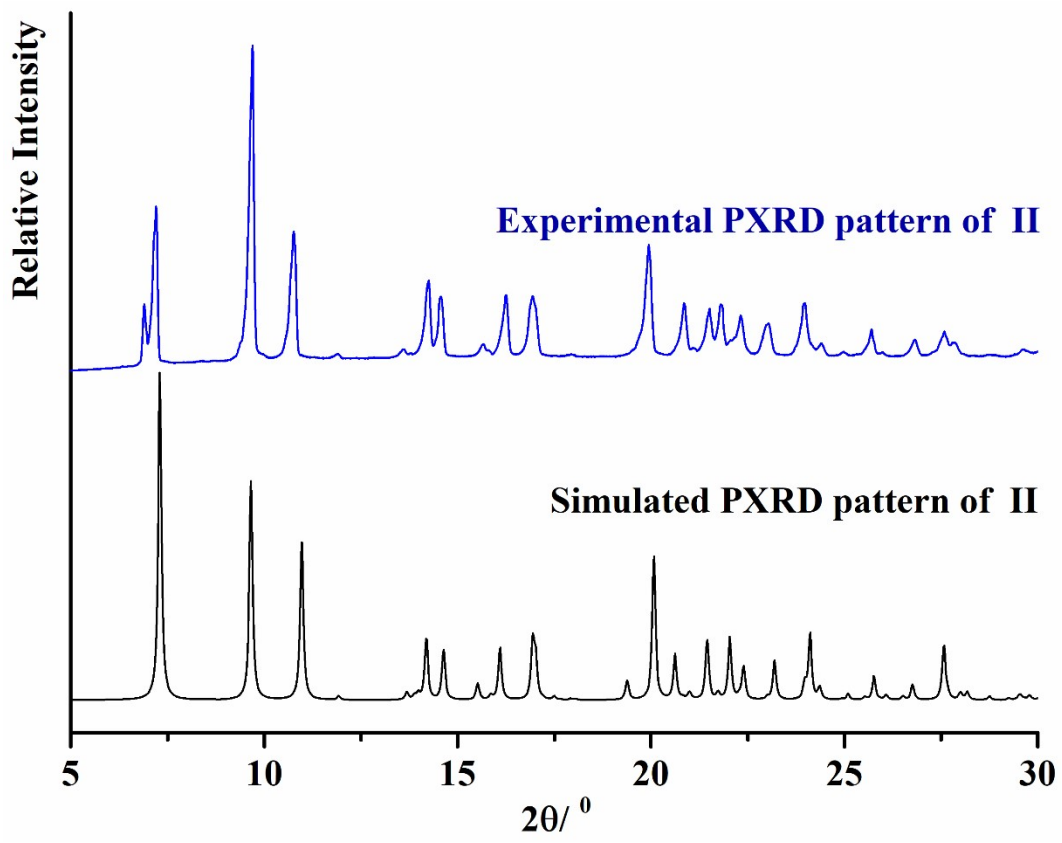

(b)

Figure S3. Diagram showing the perfect matching of the experimental and the simulated Powder X-ray diffraction patterns of: a) **I** and b) **II**.

The software Mercury was used for simulations from the X-ray structure data sets.[3] *The less intense additional peak attached to the first peak in the experimental PXRD pattern of **II** is related to its partial dehydrated phase (**II'**). Such a mismatch between simulated and experimental diffractograms was already experienced earlier by us for flexible solvent-filled frameworks* [2, 4, 5].

Section 4. Elemental analysis of both compounds

Table S4. Results from elemental analysis of **I** and **II.** *A PerkinElmer 2400 series 2 elemental analyzer was used.*

	%C		%N		%H	
	Exp	**Calc**	**Exp**	**Calc**	**Exp**	**Calc**
I	35.32	35.66	10.29	10.41	3.96	4.49
II	37.06	35.35	11.47	10.99	3.94	4.35

Section 5. Lattice parameters of the two materials at the studied humidity levels

Table S5. Values of the lattice parameters of I'/I during the adsorption of water molecules at different humidity levels

Humidity levels (%)	**Lattice parameters**				**Volumes (Å^3)**
	a (Å)	**b (Å)**	**c (Å)**	**β (º)**	
0.0	12.054	16.092	13.884	99.801	2651.649
7.5	12.069	16.151	13.893	99.896	2665.619
12.9	12.067	16.176	13.889	99.883	2668.643
17.7	12.067	16.176	13.891	99.881	2669.044
22.4	12.061	16.175	13.887	99.876	2666.826
27.7	12.067	16.195	13.888	99.911	2671.351
32.2	13.233	18.261	14.139	100.501	3356.475
37.0	13.233	18.261	14.139	100.501	3356.475
45.2	13.233	18.261	14.131	100.501	3354.576
49.5	13.243	18.267	14.141	100.588	3359.614
51.7	13.257	18.279	14.110	100.660	3357.159
56.7	13.284	18.307	14.123	100.543	3373.604
64.4	13.291	18.294	14.137	100.727	3374.234
66.4	13.276	18.297	14.129	100.637	3370.098
79.1	13.273	18.318	14.127	100.542	3373.728
81.2	13.269	18.321	14.129	100.477	3374.641
85.2	13.270	18.329	14.121	100.367	3375.589
88.1	13.263	18.329	14.124	100.276	3375.530

Table S6. Values of the lattice parameters of I'/I during the desorption of water molecules at different humidity levels

Humidity levels (%)	Lattice parameters				Volumes (Å^3)
	a (Å)	b (Å)	c (Å)	β (º)	
88.1	13.263	18.329	14.124	100.276	3375.530
86.9	13.245	18.340	14.129	100.222	3374.783
83.5	13.243	18.333	14.127	100.201	3372.712
79.9	13.240	18.325	14.126	100.186	3370.401
76.9	13.233	18.325	14.128	100.150	3369.487
61.5	13.256	18.313	14.138	100.170	3375.304
59.9	13.190	18.243	14.095	99.908	3338.267
54.4	13.185	18.236	14.956	99.908	3539.486
47.3	13.250	18.294	14.139	100.124	3371.013
44.4	13.249	18.285	14.137	100.111	3368.764
37.1	13.248	18.281	14.135	100.110	3367.307
32.1	13.246	18.275	14.134	100.105	3365.509
28.4	13.243	18.269	14.131	100.097	3363.015
22.4	13.242	18.262	14.129	100.096	3361.007
17.6	13.241	18.256	14.125	100.088	3358.784
12.7	13.241	18.256	14.125	100.088	3358.784
7.3	13.241	18.256	14.125	100.088	3358.784
0.0	12.106	16.081	13.908	99.743	2666.287

Table S7. Values of the lattice parameters of II ’/II during the adsorption of water molecules at different humidity levels

Humidity levels (%)	Lattice parameters				Volumes (Å^3)
	a (Å)	b (Å)	c (Å)	β (º)	
0.0	17.5728	16.5700	13.5958	111.4606	3684.3801
7.5	17.5990	16.5433	13.6021	111.344	3688.5447
17.7	17.499	17.877	13.751	112.592	3962.695
22.4	17.516	17.956	13.763	112.7067	3984.571
27.1	17.528	17.984	13.773	112.772	3994.463
32.2	17.530	18.033	13.777	112.866	4003.848
37.0	17.571	18.168	13.807	113.219	4041.460
45.2	17.588	18.219	13.818	113.341	4056.363
49.4	17.611	18.285	13.835	113.552	4074.359
51.7	17.607	18.296	13.834	113.600	4074.287
56.7	17.622	18.329	13.845	113.702	4085.205
64.4	17.648	18.373	13.858	113.870	4099.328
66.4	17.637	18.374	13.855	113.860	4096.421
71.1	17.642	18.391	13.859	113.897	4101.341
79.5	17.648	18.408	13.862	113.956	4105.386
81.2	17.652	18.414	13.864	113.972	4107.978
85.1	17.656	18.421	13.866	114.001	4110.377
88.1	17.657	18.428	13.867	114.015	4111.912

Table S8. Values of the lattice parameters of II 'during the desorption of water molecules at different humidity levels

Humidity levels (%)	Lattice parameters				Volumes (Å^3)
	a (Å)	b (Å)	c (Å)	β (^{o})	
88.1	17.657	18.428	13.867	114.015	4111.912
86.9	17.658	18.426	13.868	114.013	4111.883
83.5	17.655	18.417	13.865	113.983	4109.089
79.9	17.645	18.404	13.860	113.946	4103.613
76.9	17.645	18.404	13.860	113.945	4103.607
67.9	17.639	18.379	13.856	113.882	4097.494
61.5	17.630	18.349	13.851	113.791	4090.0732
59.9	17.630	18.349	13.851	113.791	4090.077
54.4	17.617	18.315	13.842	113.676	4080.649
47.3	17.603	18.272	13.830	113.539	4068.915
44.4	17.589	18.216	13. 823	113.406	4051.875
37.1	17.569	18.165	13.807	113.245	4039.469
32.1	17.557	18.113	13.797	113.056	4028.018
28.4	17.535	18.033	13.781	112.874	4006.061
22.4	17.517	17.959	13.766	112.732	3985.181
17.6	17.503	17.880	13.755	112.607	3965.0278
12.7	17.493	17.822	13.747	112.580	3948.935
0.0	17.571	16.570	13.598	111,464	3689.131

Section 6. Powder diffraction patterns of I'/I during the discontinuous phase transition

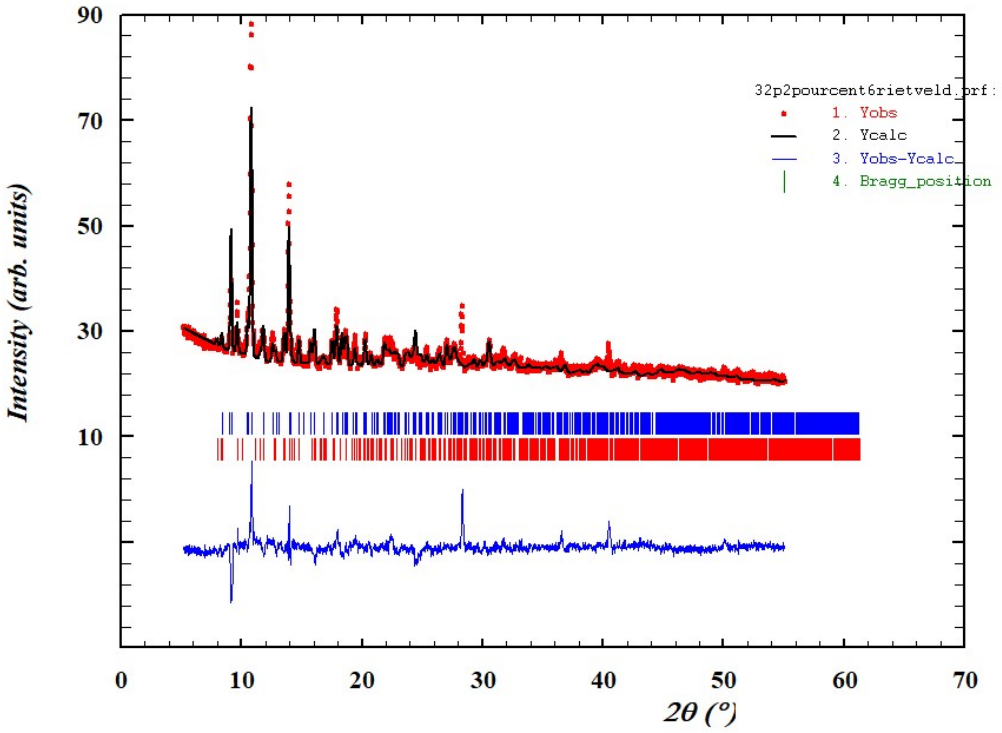

BRAGG R-Factors and weight fractions for Pattern # 1

=> Phase: 1 **I'**

=> Bragg R-factor: 28.7 Vol: 2723.615(3.551) Fact (%): 82.07(5.83)

=> Rf-factor= 19.5 ATZ: 2797.669 Brindley: 1.0000

=> Phase: 2 **I**

=> Bragg R-factor: 33.7 Vol: 3379.703(15.118) Fact (%): 17.93(3.84)

=> Rf-factor= 21.4 ATZ: 3230.040 Brindley: 1.0000

Figure S4. Powder diffraction patterns of **I'/I** at 32.2 % r.H. and values of agreement parameters obtained with Rietveld refinement.

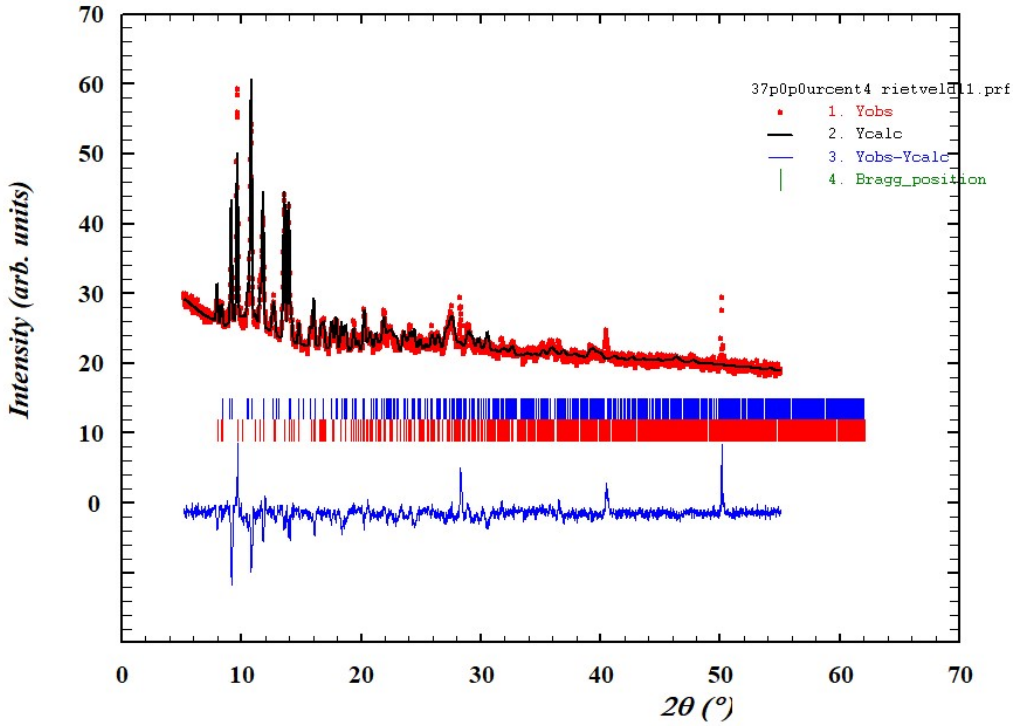

BRAGG R-Factors and weight fractions for Pattern # 1

=> Phase: 1 **I'**

=> Bragg R-factor: 42.6 Vol: 2725.223(4.547) Fract(%): 45.22(4.79)

=> Rf-factor= 20.9 ATZ: 2797.669 Brindley: 1.0000

=> Phase: 2 **I**

=> Bragg R-factor: 22.7 Vol: 3374.759(6.222) Fract(%): 54.78(5.56)

=> Rf-factor= 16.5 ATZ: 3230.040 Brindley: 1.0000

Figure S5. Powder diffraction patterns of **I'/I** at 37.7 % r.H. and values of agreement parameters obtained with Rietveld refinement.

References

1. P. K. Tsobnang, J. L. Ngolui, E. Wenger, P. Durand, S. Dahaoui, C. Lecomte, *Cryst. Growth Des.,* 2017, **17,** 4908 – 4917.
2. P. K. Tsobnang, E. Hastürk, D. Fröhlich, E. Wenger, P. Durand, J. N. Lambi, C. Lecomte, C. Janiak, *Cryst. Growth Des*., 2019, **19**, 2869 – 2880.
3. Mercury 4.0: from visualization to analysis, design and prediction C. F. Macrae, I. Sovago, S. J. Cottrell, P. T. A. Galek, P. McCabe, E. Pidcock, M. Platings, G. P. Shields, J. S. Stevens, M. Towler and P. A. Wood, J. Appl. Cryst., **53**, 226 – 235, 2020.
4. S. Glomb, G. Makhloufi; I. Gruber, C. Janiak, *Inorg. Chim. Acta***,** 2018, **475**, 35 – 46.
5. S. Glomb, D. Woschko, G. Makhloufi, C. Janiak, *ACS Appl. Mater. Interfaces.,* 2017, **9**, 37419 – 37434.